Synthesis of silyl iron dinitrogen complexes for activation of dihydrogen and catalytic silylation of dinitrogen†

Guoliang Chang,[a] Peng Zhang,[a] Wenjing Yang,[a] Yanhong Dong,[a] Shangqing Xie,[a] Hongjian Sun,[a] Xiaoyan Li,*[a] Olaf Fuhr[b] and Dieter Fenske[b]

Three novel iron dinitrogen hydrides, [FeH(^{i}Pr-PSi^{Me}P)(N_2)(PMe_3)] (**1**), [FeH(^{i}Pr-PSi^{Ph}P)(N_2)(PMe_3)] (**2**), and [FeH(^{i}Pr-PSi^{Ph})(N_2)(PMe_3)] (**3**), supported by a silyl ligand are synthesized for the first time by changing the electronic effect and steric hindrance of the ligands through the reaction of ligands **L1–L3** with $Fe(PMe_3)_4$ in a nitrogen atmosphere. The ligands containing an electron-donating group with large steric hindrance on the phosphorus atom are beneficial for the formation of dinitrogen complexes. A penta-coordinate iron hydride [FeH(^{i}Pr-PSi^{Ph})(PMe_3)$_2$] (**4**) was formed through the reaction of ligand **L3** with $Fe(PMe_3)_4$ in an argon atmosphere under the same conditions. The reactions between complexes **1–3** with an atmospheric pressure of dihydrogen gas resulted in Fe(II) dihydrides, [(^{i}Pr-PSi^{Me}(μ-H)P)$Fe(H)_2(PMe_3)$] (**5**), [(^{i}Pr-PSi^{Ph}(μ-H)P)$Fe(H)_2(PMe_3)$] (**6**) and [(iPr-PSi^{Ph}(μ-H))$Fe(H)_2(PMe_3)_2$] (**7**), with an η^2-(Si–H) coordination. The isolation of dihydrides **5–7** demonstrates the ability of the dinitrogen complexes **1–3** to realize the activation of dihydrogen under ambient temperature and pressure. The molecular structures of complexes **1–7** were elucidated by single crystal X-ray diffraction analysis. The iron dinitrogen hydrides **1–3** are effective catalysts for the silylation of dinitrogen under ambient conditions and among them **3** is the best catalyst.

Introduction

It is well known that iron-containing catalysts are used in Haber–Bosch ammonia synthesis and the active center of nitrogenase contains iron.[1,2] Therefore, when studying the nitrogen fixation promoted by transition metal complexes, chemists pay great attention to the synthesis and application of iron-containing complexes.[3] In various forms of nitrogen fixation, the silylation of nitrogen is one of the reduction methods of nitrogen.

The first successful example of Fe-catalyzed transformation of N_2 into $N(SiMe_3)_3$ under ambient conditions was disclosed by Nishibayashi in 2012.[4] The formation of $N(SiMe_3)_3$ from N_2 could also be catalyzed by two-coordinate NHC iron(0) complexes.[5] In 2017, Mock reported that the square pyramidal Fe$(N_2)(P_4N_2)$ complex catalyzed the conversion of N_2 to $N(SiR_3)_3$ at room temperature with a TON of 65 equiv. $N(SiMe_3)_3$ per Fe atom.[6] [PSiP] pincer iron(II) nitrogen complexes were used as catalysts for the catalytic silylation of nitrogen gas into silylamine under ambient reaction conditions.[7] The reduction of dinitrogen to $N(SiMe_3)_3$ was promoted with a series of triiron complexes supported by tris(β-diketiminate)cyclophanes as catalysts.[8] Ashley demonstrated that complexes $Fe(PP)_2(N_2)$ (PP = $R_2PCH_2CH_2PR_2$, R = Me and Et) are highly effective for the catalytic production of $N(SiMe_3)_3$ from N_2 and discussed the possible catalytic mechanism for the reductive silylation of N_2 based on experimental results and DFT calculations.[9] Recently, our group realized the silylation of nitrogen at room temperature and atmospheric pressure using a bis(silylene)-based [SiCSi] pincer dinitrogen iron(II) hydride as the catalyst.[10] So far, although a lot of work has been published in this field, no practical nitrogen reduction catalyst has been found.

As we know, the properties of metal complexes can be regulated by the properties of the ligands. In recent years, silyl [P,Si] chelate ligands have attracted more and more attention because of their strong electron-donating ability and *trans*-influence effects, which can improve the catalytic activity of

[a]*School of Chemistry and Chemical Engineering, Key Laboratory of Special Functional Aggregated Materials, Ministry of Education, Shandong University, Shanda Nanlu 27, 250100 Jinan, People's Republic of China. E mail: xli63@sdu.edu.cn*

[b]*Institut für Nanotechnologie (INT) und Karlsruher Nano Micro Facility (KNMF), Karlsruher Institut für Technologie (KIT), Hermann von Helmholtz Platz 1, 76344 Eggenstein Leopoldshafen, Germany*

†Electronic supplementary information (ESI) available: The table of selected crystallographic data and original IR, ^{1}H, ^{31}P, ^{13}C and ^{29}Si NMR spectra of com plexes **1** 7. CCDC 1561102 (**1**), 1918904 (**2**), 1909697 (**3**), 1936213 (**4**), 1971373 (**5**), 1972115 (**6**) and 1972114 (**7**). For ESI and crystallographic data in CIF or other electronic format see DOI: 10.1039/d1dt02832d

the metal complex.[11] Inspired by the work by Peters' and Nishibayashi's group,[7] we incorporated isopropyl groups into the ligands in order to synthesize silyl iron dinitrogen complexes with better catalytic effects for the reduction of nitrogen to form silylamine under mild reaction conditions.

Results and discussion

Preparation of silyl chelate iron dinitrogen complexes 1–3

The reaction of ligand **L1** (bis(*o*-(diisopropylphosphino) phenyl)methylsilane) or **L2** (bis(*o*-(diisopropylphosphino) phenyl)phenylsilane) with $Fe(PMe_3)_4$ afforded silyl [PSiP] pincer iron nitrogen hydride **1** or **2** in a yield of 75% (**1**) or 59% (**2**) (Scheme 1).

In the IR spectra of complexes **1** and **2**, both the absorption of N≡N bonds and Fe–H vibrations were registered at 2052 (**1**)/2067 (**2**) cm^{-1} and 1924 (**1**)/1873 (**2**) cm^{-1}, respectively. Compared to that of complex **1**, the signal of N≡N of complex **2** shows a hypsochromic shift. It is considered that the replacement of methyl with phenyl reduces the density of the electron cloud on the central iron atom, which weakens the π-backdonation between the Fe center and N≡N ligand, resulting in this shift. The ^1H NMR spectrum of **1** shows a "td" signal at −14.91 ppm for the hydrido ligand, formed by (PH)-coupling with three P atoms (J_{PH} = 24 and 69 Hz). In the ^{31}P NMR spectrum of **1**, two signals appear at 23.2 and 106.3 ppm in the integral ratio of 1 : 2, assigned to the PMe_3 ligand and -P^iPr_2 group, respectively. The NMR spectra of complex **2** are similar to those of complex **1** (see the ESI†). The ^{29}Si NMR signals for complexes **1** and **2** were found at 60.2 and 65.8 ppm, respectively.

The molecular structure of **1** was confirmed by single crystal X-ray diffraction analysis. Complex **1** has a distorted octahedral geometry with the iron atom in the center (Fig. 1). The axial angle of N1–Fe1–Si1 is 164.29(1)°, deviated from 180°. The equatorial plane is occupied by [P1P2P3H1Fe1] with the sum (360.6°) of the coordinate bond angles (P1–Fe1–H1 (72(1)°), P1–Fe1–P3 (103.43(4)°), P2–Fe1–P3 (105.19(4)°) and P2–Fe1–H1 (80(1)°). The length of Fe1–H1 is 1.50(3) Å. The length of N1–N2 (1.161(5) Å) is longer than those of similar complexes.[7,10,12] This indicates that the activation of the N≡N bond in complex **1** is stronger than those in similar complexes.[7] Fe1–P3 (2.2408(1) Å) is longer than Fe1–P1 (2.2102(9) Å) and Fe1–P2 (2.2245(9) Å) because of the strong *trans*-influence of the hydrido ligand. Complex **2** (Fig. 2) has a similar molecular structure to complex **1** but N≡N (1.107(3) Å) in complex **2** is slightly shorter than that (1.161(5) Å) of complex **1** due to the replacement of the methyl group with the phenyl group. This result is consistent with that of the infrared spectrum. The Fe1–HA bond (1.47(4) Å) in complex **2** is almost the same as Fe1–H1 (1.50(3) Å) in complex **1**. Compared to our early published complex,[13] it is found that the replacement of the phenyl with the isopropyl group is beneficial for the formation of the dinitrogen complex. We think that the introduction the isopropyl groups increases the electron cloud density at the iron center, which enhances the π-backdonation from Fe to N_2.

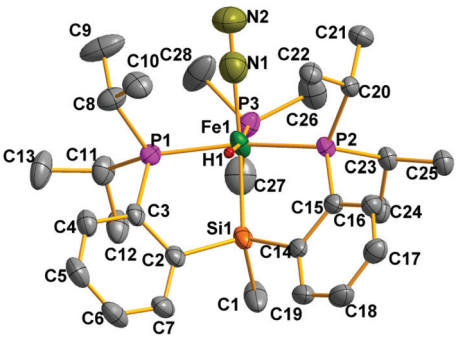

Fig. 1 ORTEP plot of complex **1** at the 50% probability level (most of the hydrogen atoms are omitted for clarity). Selected bond lengths (Å) and angles (deg): Fe1 P1 2.2102(9), Fe1 P2 2.2245(9), Fe1 P3 2.2408(1), Fe1 Si1 2.3152(1), Fe1 N1 1.880(4), Fe1 H1 1.50(3), N1 N2 1.161(5); P1 Fe1 P2 151.25(4), P1 Fe1 P3 103.43(4), P2 Fe1 P3 105.19(4), P1 Fe1 Si1 83.77(3), P3 Fe1 Si1 112.29(4), N1 Fe1 Si1 164.29(1), N2 N1 Fe1 179.4(4).

Intrigued by the interesting reaction of [PSiP] pincer ligand **L1** or **L2** and $Fe(PMe_3)_4$ as well as other reported [PSiP] pincer

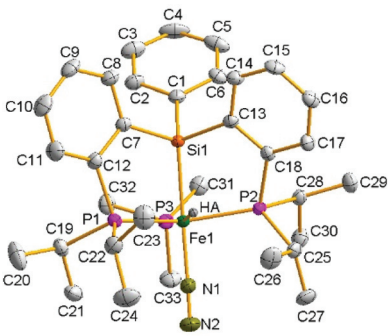

Fig. 2 ORTEP plot of complex **2** at the 50% probability level (most of the hydrogen atoms are omitted for clarity). Selected bond lengths (Å) and angles (deg): Fe2 P62 2.2300(7), Fe1 P2 2.2282(7), Fe1 P1 2.2398(8), Fe1 Si1 2.2986(7), Fe1 P3 2.2564(8), Fe1 N1 1.838(2), N1 N2 1.107(3), Fe1 HA 1.47(4); P2 Fe1 P1 142.18(3), P2 Fe1 Si1 83.54(3), P2 Fe1 P3 109.17(3), P1 Fe1 Si1 84.81(3), P1 Fe1 P3 107.10(3), P3 Fe1 Si1 92.11(3), N1 Fe1 P2 95.07(7), N1 Fe1 P1 93.90(8), N1 Fe1 Si1 175.71(8), N1 Fe1 P3 92.18(8), P2 Fe1 HA 70(2), P1 Fe1 HA 72(2), Si1 Fe1 HA 78(2), P3 Fe1 HA 170(2), N1 Fe1 HA 98(2).

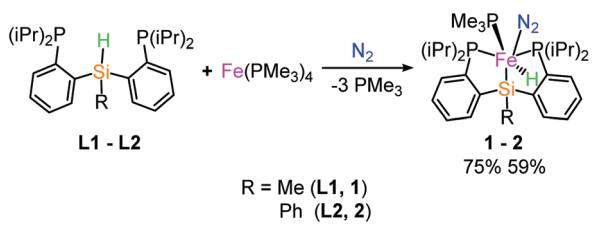

Scheme 1 Preparation of complexes **1** and **2**.

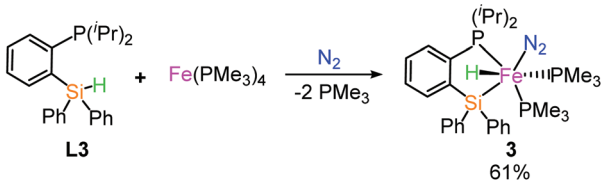

Scheme 2 Preparation of complex **3**.

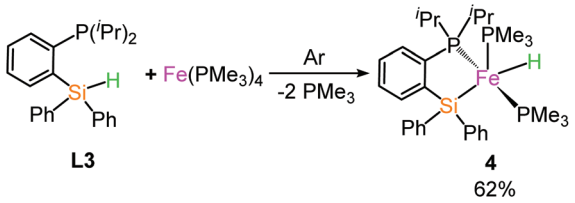

Scheme 3 Preparation of complex **4**.

dinitrogen complexes,[7,14] we were also curious about the reaction between [P,Si] bidentate ligand **L3** and $Fe(PMe_3)_4$ (Scheme 2). As expected, the hexa-coordinate [P,Si] chelate iron (II) nitrogen hydride **3** was formed from the reaction of **L3** with $Fe(PMe_3)_4$. In the IR spectrum of **3** the typical signal for the N≡N bond is situated at 2054 cm^{-1} while the stretching band for the Fe–H bond is registered at 1902 cm^{-1}. In the ^1H NMR spectrum of **3** the hydrido resonance appears at −11.23 ppm as a "td" peak with J_{PH} = 25 and 64 Hz. The ^{29}Si NMR signal for complex **3** was found at 48.6 ppm.

The molecular structure of **3** was confirmed by single crystal X-ray diffraction analysis (Fig. 3). Complex **3** has a distorted octahedral geometry around the iron atom. The Fe1–H bond (1.51 Å) is almost as long as those of complexes **1** and **2**. The bond length of N1–N2 (1.130 Å) lies in the range of those of reported terminal nitrogen Fe complexes (1.101–1.154 Å).[6–9,12]

In order to exclude the influence of nitrogen on the reaction of **L3** with $Fe(PMe_3)_4$, the reaction of ligand **L3** with $Fe(PMe_3)_4$ was carried out in atmospheric argon under the same conditions. Interestingly, a penta-coordinate iron hydride **4** was formed (Scheme 3). The typical Fe–H vibration was found at 1892 cm^{-1} in the IR spectrum of **4** while the hydrido resonance of **4** was observed at −12.42 ppm in the ^1H NMR spectrum of **4**. Single crystal X-ray diffraction analysis confirms

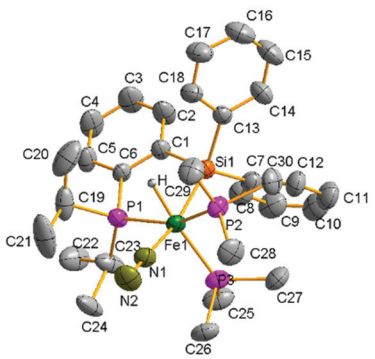

Fig. 3 ORTEP plot of complex **3** at the 50% probability level (most of the hydrogen atoms are omitted for clarity). Selected bond lengths (Å) and angles (deg): Fe1 P1 2.251(1), Fe1 Si1 2.347(1), Fe1 P2 2.215(1), Fe1 P3 2.254(1), Fe1 N1, 1.832(4). N1 N2 1.130(5), Fe1 H1 1.51(1); Si1 Fe1 H 76(2), P3 Fe1 H 174(2), P1 Fe1 H 73(2), P2 Fe1 H 84(2), N1 Fe1 H 93(2), P1 Fe1 Si1 84.58(4), P1 Fe1 P3 109.24(5), P2 Fe1 P1 156.07(5), P2 Fe1 Si1 93.49(5), P2 Fe1 P3 94.64(5), P3 Fe1 Si1 98.60(5), N1 Fe1 P1 90.9(1), N1 Fe1 Si1 168.4(1), N1 Fe1 P2 86.3(1), N1 Fe1 P3 93.0(1).

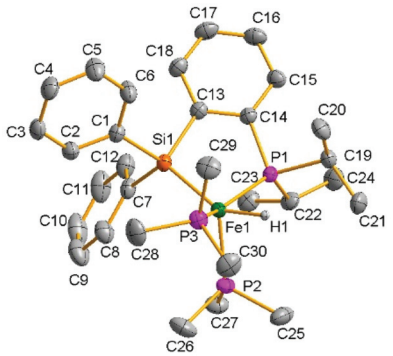

Fig. 4 ORTEP plot of complex **4** at the 50% probability level (most of the hydrogen atoms are omitted for clarity). Selected bond lengths (Å) and angles (deg): Fe1 P1 2.1943(4), Fe1 P2 2.2051(4), Fe1 P3 2.1745(4), Fe1 Si1 2.2816(4), Fe1 H1 1.52(2); P1 Fe1 P2 102.23(2), P1 Fe1 Si1 84.07(1), P2 Fe1 Si1 119.12(2), P3 Fe1 P1 143.56(2), P3 Fe1 P2 99.31(2), P3 Fe1 Si1 110.31(2), H1 Fe1 P1 78.1(7), H1 Fe1 P2 88.1(7), H1 Fe1 P3 73.6(7), H1 Fe1 Si1 150.3(7).

that complex **4** has a distorted penta-coordinate tetragonal pyramidal geometry with the geometric index τ = 0.11 (where τ = 0.00 for a perfect tetragonal pyramid and τ = 1.00 for a trigonal bipyramidal geometry)[15] (Fig. 4). The bond of Fe1–H1 (1.52(2) Å) is comparable to those of complexes **1–3**.

The bis(silylene) [SiCSi] pincer preligand reacted with Fe $(PMe_3)_4$ under N_2 to give rise to the first example of a transition metal dinitrogen complex supported by a bis(silylene) ligand while the same reaction was carried out under Ar to deliver a six-coordinated iron hydride.[10] The replacement of the tridentate [SiCSi] ligand with the bidentate [P,Si] ligand changes the product from (low-spin) hexa-coordination to (high-spin) penta-coordination. It is considered that both the steric hindrance and electronic effect play a role.

Comparing complexes **1–3** with silyl [P,Si] chelate iron complexes **1a–1e**,[13,16] **1f–1g**[7] and **2a–2d**[17] in the literature, it is found that the substituents on the ligands have a great influence on the formation of nitrogen complexes. This effect is related not only to the electronic properties of the ligands, but also to the steric hindrance of the ligands (Scheme 4). When the P atom is connected to iPr and the Si atom is connected to the Me- /Ph-group with the increase of electron cloud density at the central iron atom, it is conducive to the formation of nitrogen complexes with the π-backbond (Scheme 4). When P is connected with the Ph-group, it is not conducive to the for-

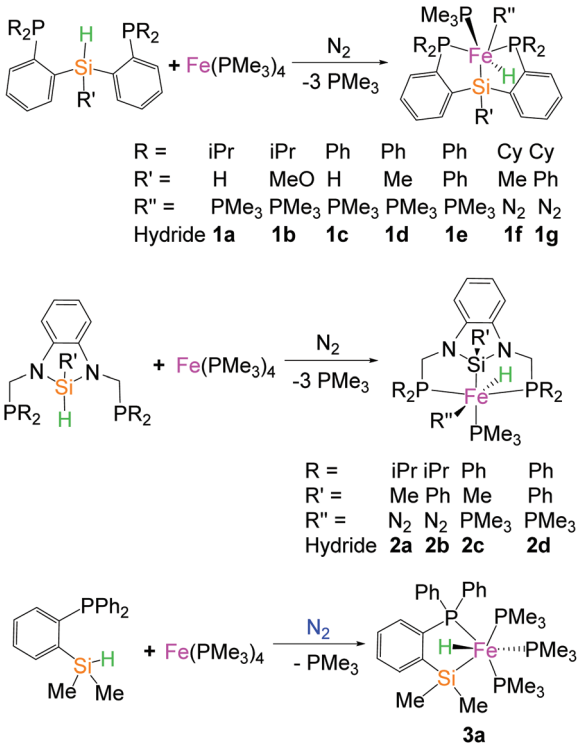

Scheme 4 The effect of ligands on the formation of dinitrogen complexes.

mation of the π-backbond and nitrogen complex. For complex **3a**,[18] no nitrogen complex was formed because the phenyl groups are on the P atom.

The hydrogenation of the dinitrogen complexes

The activation of dihydrogen under ambient conditions is an important challenge for the investigation of the mechanisms of hydrogenation reactions. Normally dinitrogen in the dinitrogen complexes is easily dissociated forming coordinate unsaturated species. It is obvious that the nitrogen complexes can be used for the activation of dihydrogen.[14]

The reaction between complex **1** or **2** with atmospheric pressure of dihydrogen gas resulted in the formation of Fe(II) dihydride **5** or **6** with an η^2-(Si–H) coordination under ambient temperature in 68% (**5**) or 62% (**6**) yield (Scheme 5). In the IR

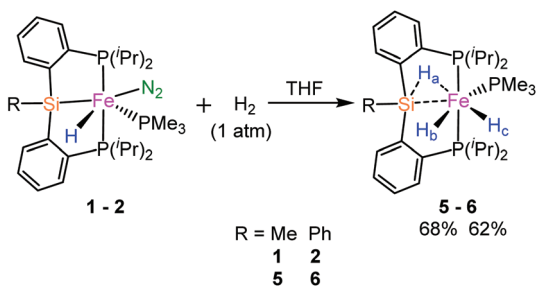

Scheme 5 Preparation of complexes **5 and 6**.

spectrum of **5**, there are three strong signals at 2057, 1919 and 1836 cm^{-1}, caused by the Si–H and Fe–H bonds.[19] In the ^1H NMR spectrum of **5**, two broadened characteristic signals appear at −10.03 (Ha and Hb) and −15.01 (Hc) ppm in the integral ratio of 2 : 1. It is considered that there is fast exchange between Ha and Hb in the solution at ambient temperature. This result is similar to that of the iron hydride reported by Turculet.[14] Single crystal X-ray diffraction analysis verifies that complex **5** has a distorted hexa-coordinate octahedral geometry, featuring *mer*-[PSiP] pincer coordination with an η^2-(Si–H) coordination as a ligand (Fig. 5). When P3–Fe1–H

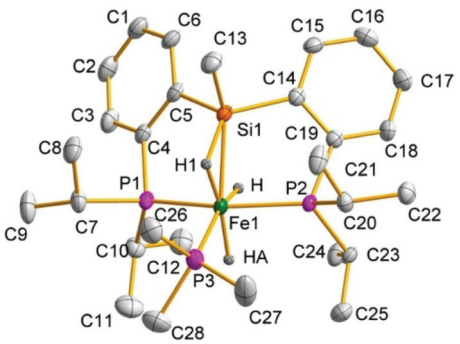

Fig. 5 ORTEP plot of complex **5** at the 50% probability level (most of the hydrogen atoms are omitted for clarity). Selected bond lengths (Å) and angles (deg): Fe1 P1 2.1881(7), Fe1 P2 2.1916(7), Fe1 Si1 2.2890(7), Fe1 P3 2.2178(7), Fe1 H1 1.49(3), Fe1 H 1.36(2), Fe1 HA 1.49(3); P1 Fe1 P2 150.17(3), P1 Fe1 Si1 86.99(3), P1 Fe1 P3 102.37(3), P2 Fe1 Si1 85.65(3), P2 Fe1 P3 104.80(3), P3 Fe1 Si1 128.59(3), P1 Fe1 H1 97(1), P1 Fe1 H 76(1), P1 Fe1 HA 85(1), P2 Fe1 H1 100(1), P2 Fe1 H 74(1), P2 Fe1 HA 86(1), P3 Fe1 H1 81(1), P3 Fe1 H, 163(1), P3 Fe1 HA 82(1), H1 Fe1 H 116(2), H1 Fe1 HA 163(2), H Fe1 HA 81(2).

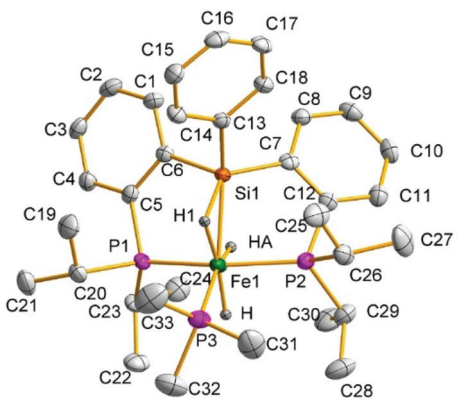

Fig. 6 ORTEP plot of complex **6** at the 50% probability level (most of the hydrogen atoms are omitted for clarity). Selected bond lengths (Å) and angles (deg): Fe1 P1 2.190(1), Fe1 P2 2.197(1), Fe1 Si1 2.2771(9), Fe1 P3 2.217(1), Fe1 H 1.41(3), Fe1 HA 1.42(4), Fe1 H1 1.48(4); P1 Fe1 P2 150.72(4), P1 Fe1 Si1 87.59(3), P1 Fe1 P3 102.42(4), P2 Fe1 Si1 84.57(3), P2 Fe1 P3 103.38(4), P3 Fe1 Si1 133.59(4), P1 Fe1 H 86(1), P1 Fe1 HA 74(1), P1 Fe1 H1 95(2), P2 Fe1 H 85(1), P2 Fe1 HA 77(1), P2 Fe1 H1 101(2), P3 Fe1 H 80(1), P3 Fe1 HA 160(1), P3 Fe1 H1 86(2), H Fe1 HA 80(2), H Fe1 H1 165(2), HA Fe1 H1 114(2).

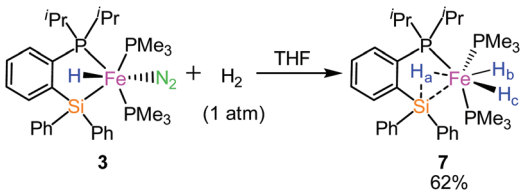

Scheme 6 Preparation of complex **7**.

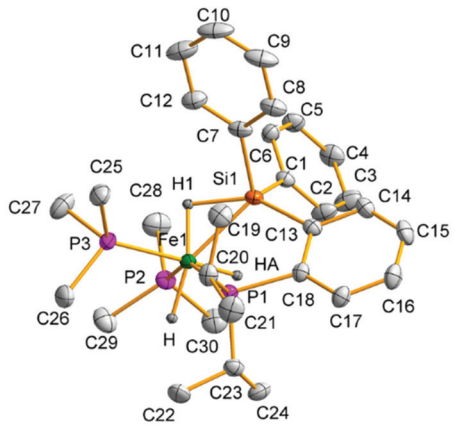

Fig. 7 ORTEP plot of complex **7** at the 50% probability level (most of the hydrogen atoms are omitted for clarity). Selected bond lengths (Å) and angles (deg): Fe1 P1 2.1959(7), Fe1 P2 2.1758(7), Fe1 P3 2.2060(7) Fe1 Si1 2.2827(7), Fe1 H1 1.47(3), Fe1 H 1.47(3), Fe1 HA 1.38(4); P1 Fe1 P3 102.11(3), P1 Fe1 Si1 84.08(3), P2 Fe1 P1 143.70(3), P2 Fe1 P3 99.34(3), P2 Fe1 Si1 110.27(3), P3 Fe1 Si1 119.08(3), P1 Fe1 H1 124(1), P1 Fe1 H 79(1), P1 Fe1 HA 80(1), P2 Fe1 H1 88(1), P2 Fe1 H 72(1), P2 Fe1 HA 78(1) P3 Fe1 H1 83(1), P3 Fe1 H 89(1) P3 Fe1 HA 177(1), H1 Fe1 H 157(2), H1 Fe1 HA 98(2), H Fe1 HA 89(2).

(163(1)°) is axial, the equatorial plane is formed by [P1,HA, P2, A (the middle point of the Si–H bond) and Fe1]. The sum of the coordination bond angles in the equatorial plane (P1–Fe1–HA (85(1)°), P2–Fe1–HA (86(1)°), P1–Fe1–A (90.86(3)°) and P2–Fe1–A (91.26(2)°) is 353°, deviated from 360°. It is noteworthy that the acute angle Si1–Fe1–H1 (48.1°) indicates an interaction between Si1 and H1. Moreover, the sum of the van der Waals radii of the Si and H atoms (3.4 Å) is much longer than the distance of Si1–H1 (1.70(3) Å). This further demonstrates the interaction between Si1 and H1. Si1–H (2.1819 Å) between 1.9 and 2.4 Å indicates a possible secondary interaction between Si1 and the H atom.[14] In addition, the bond of Si1–H1 (1.70(3) Å) is obviously longer than that of the parent silane (~1.5 Å). This verifies that the Si–H1 bond is activated by the iron center. These metrical parameters reveal that complex **5** has an η^2-(Si–H) coordination with the presence of SISHA (secondary interaction between a Si and a H atom).[14,20] Complex **6** (Fig. 6) with complex **5** has similar spectroscopic and structural characteristics (see the ESI†).

As [PSiP] pincer complexes **1** and **2**, chelate complex **3** could also activate dihydrogen to convert to iron dihydride **7** with an η^2-(Si–H) coordination under the same conditions (Scheme 6). Single crystal X-ray diffraction analysis further confirms the structure of complex **7** (Fig. 7). Complex **7** also exhibits a distorted octahedral geometry with a central iron atom. The equatorial plane contains P1, P2, H, Fe1 and the middle point of the H1–Si1 bond. The axial is occupied by P3–Fe1–HA (177°). Fe1–P3 (2.2060(8) Å) is slightly longer than Fe1–P1 (2.1960(7) Å) and Fe1–P2 (2.1758(8) Å) due to the strong *trans*-influence of HA. Otherwise, compared with the related bond parameters of complexes **5** and **6**, complex **7** is also an iron dihydride with an η^2-(Si–H) coordination.

Table 1 Catalytic silylation of N_2 with complexes **1–3** [a]

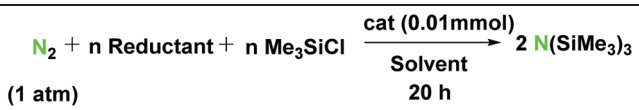

Entry	Catalyst	Reductant	Solvent	T (°C)	Reductant/Me_3SiCl (equiv.)[b]	$N(SiMe_3)_3$ (equiv.)[b,c]
1	**1**	KC_8	Dioxane	25	600	15.2
2	**2**	KC_8	Dioxane	25	600	17.9
3	**3**	KC_8	Dioxane	25	600	21.4
4	**3**	K	Dioxane	25	600	3.7
5	**3**	Na	Dioxane	25	600	2.8
6	**3**	Li	Dioxane	25	600	0.9
7	**3**	KC_8	THF	25	600	18.2
8	**3**	KC_8	Toluene	25	600	11.1
9	**3**	KC_8	DMF	25	600	7.8
10	**3**	KC_8	DMSO	25	600	3.4
11	**3**	KC_8	Et_2O	25	600	13.4
12	**3**	KC_8	Dioxane	0	600	10.2
13	**3**	KC_8	Dioxane	50	600	10.9
14	**3**	KC_8	Dioxane	80	600	3.9
15	**3**	KC_8	Dioxane	25	1800	49.1
16[d]	**3**	KC_8	Dioxane	25	1800	78.2
17		KC_8	Dioxane	25	1800	0

[a] Experiments performed over 20 h in 20 mL of solvent using a 0.01 mmol catalyst under N_2, unless otherwise stated. Yields are an average of 2 trials. [b] Based on the catalyst. [c] Determined by GC. [d] Conducted for 150 h.

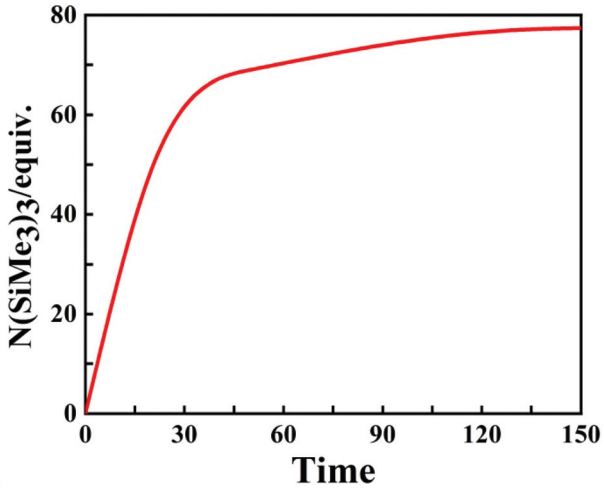

Fig. 8 Time profile of the formation of $N(SiMe_3)_3$ using **3** as the catalyst.

Catalytic silylation of N_2 using 1–3 as catalysts

At the beginning, the catalytic reaction was performed with complex **1** as a catalyst, combining with KC_8 (600 equiv. based on **1**) and Me_3SiCl (600 equiv. based on **1**) under dinitrogen (1 atm) at room temperature for 20 h and 15.2 equiv. of $N(SiMe_3)_3$ were obtained in dioxane (entry 1, Table 1). When complex **1** was replaced with **2** or **3**, the yield of $N(SiMe_3)_3$ was increased significantly under the same reaction conditions, respectively (entries 2 and 3, Table 1) and complex **3** is the best catalyst. The experiments show that the catalytic effects are not good with Li, Na or K as a reducing agent (entries 4–6, Table 1). It is worth noting that dioxane is the best medium for this process, compared to THF, toluene, DMF, DMSO and Et_2O (entries 7–11, Table 1). However, the catalytic effect became worse when the reaction temperature was increased or decreased (entries 12–14, Table 1). With the increase of the amount of KC_8 and Me_3SiCl, the amount of $N(SiMe_3)_3$ increased remarkably (entry 15, Table 1). When we extended the reaction time to 150 h in the presence of 1800 equiv. of KC_8 and Me_3SiCl, 78.2 equiv. of $N(SiMe_3)_3$ per Fe atom were obtained (entry 16, Table 1). Complex **3** has almost similar catalytic activity to our reported bis(silylene)-based [SiCSi] pincer hydrido iron(II) dinitrogen complex for the silylation of N_2.[10] The reaction could not take place without a catalyst (entry 17, Table 1).

In order to further understand the reaction process, we monitored the relationship of time and yield of $N(SiMe_3)_3$ using complex **3** as a catalyst (see the ESI† for details) (Fig. 8). Fig. 8 shows that at the beginning of the reaction, the catalytic formation of $N(SiMe_3)_3$ increased rapidly and as the reaction proceeded, the rate of reaction gradually slowed down. The reaction was almost completed after 150 h. This is similar to our reported work.[10]

Conclusion

In summary, three novel silyl iron dinitrogen hydrides **1–3** were successfully synthesized. The ligands containing an electron-donating group with large steric hindrance on the phosphorus atom are beneficial for the synthesis of dinitrogen complexes. This is consistent with Nishibayashi's conclusion.[7] This indicates that the ligands play an important role in the preparation of dinitrogen complexes. A penta-coordinate iron hydride (**4**) was formed through the reaction of ligand **L3** with $Fe(PMe_3)_4$ in atmospheric argon under the same conditions. The reactions between complexes **1–3** with an atmospheric pressure of dihydrogen gas resulted in Fe(II) dihydrides **5–7** with an η^2-(Si–H) coordination. The isolation of dihydrides **5–7** demonstrates the ability of the dinitrogen complexes to realize the activation of dihydrogen under ambient temperature and pressure. Meanwhile, complexes **1–3** exhibited good catalytic performances for the silylation of dinitrogen. This further promoted and expanded the development of nitrogen fixation at room temperature. Nevertheless, much work remains to be done on the mechanism.

Experimental section

General procedures and materials

All manipulations were carried out under a N_2 (or Ar) atmosphere with the standard Schlenk techniques. Solvents were treated through distillation from Na-benzophenone. Infrared spectra (4000–400 cm^{-1}) were recorded on a Bruker ALPHA FT-IR instrument by using nujol mulls between KBr disks. ^1H, $^{31}P\{H\}$, $^{13}C\{H\}$ and $^{29}Si\{H\}$ NMR spectra were recorded on Bruker Avance 300 and 400 MHz spectrometers. GC analysis was realized on a Fuli 9790 chromatograph. Melting points (m.p.) were measured on a WRR instrument with the samples in sealed capillaries. $Fe(PMe_3)_4$,[21] bis(*o*-(diisopropylphosphino) phenyl)methylsilane (**L1**),[11b] bis(*o*-(diisopropylphosphino) phenyl)phenylsilane (**L2**)[22] and *o*-(diisopropylphosphino) phenyl diphenylsilane (**L3**)[19] were prepared according to the literature.

Synthesis of complex 1

Under 1 atm N_2, $Fe(PMe_3)_4$ (0.63 g, 1.75 mmol) in 30 mL of toluene was added into a solution of ligand **L1** (0.72 g, 1.67 mmol) in 30 mL of toluene at 0 °C. The mixture was stirred and warmed slowly to room temperature. The solution was evaporated at reduced pressure. The residue was extracted with *n*-pentane (60 mL) and diethyl ether (60 mL). The red orange crystals (complex **1**) were recrystallized in diethyl ether in a yield of 75% (0.84 g, 1.42 mmol). Dec.: >130 °C. Anal. Calc. for $C_{28}H_{49}FeN_2P_3Si$ (590.55 g mol^{-1}): C, 56.95; H, 8.36; N, 4.74. Found: C, 57.27; H, 8.29; N, 4.59. IR (Nujol mull, cm^{-1}): 2052 (N≡N), 1924(Fe–H), 946 (PMe_3). ^1H NMR (300 MHz, C_6D_6, 300 K, δ/ppm): −14.91 (td, J = 24 Hz, J = 69 Hz, 1H, Fe–*H*), 0.61 (q, J = 6 Hz, PCHC*H*$_3$, 6H), 0.88 (q, J = 6 Hz, PCHC*H*$_3$, 6H), 1.11 (q, J = 6 Hz, PCHC*H*$_3$, 6H), 1.11 (d, J = 6 Hz, PC*H*$_3$, 9H), 1.27 (s, C*H*$_3$, 3H), 1.39 (q, J = 6 Hz, PCHC*H*$_3$, 6H), 1.99 (m, PC*H*CH$_3$, 2H), 2.78 (m, PC*H*CH$_3$, 2H), 6.98 (q, J = 6 Hz, 2H, Ar–*H*), 7.11 (q, J = 6 Hz, 4H, Ar–*H*), 8.07 (d, J = 9 Hz, 2H, Ar–*H*). ^{31}P NMR (121 MHz, C_6D_6, 300 K, δ/ppm): 23.2 (t, J = 18 Hz, 1P,

*P*Me$_3$), 106.3 (dd, J = 6 Hz, J = 18 Hz, 2P, *P*^{i}Pr). ^{13}C NMR (75 MHz, C_6D_6, 300 K, δ/ppm): 5.7 (s, Si–*C*H$_3$), 16.0 (t, J = 2 Hz, PCH*C*H$_3$), 16.4 (t, J = 3 Hz, PCH*C*H$_3$), 17.7 (t, J = 2 Hz, PCH*C*H$_3$), 18.7 (t, J = 3 Hz, PCH*C*H$_3$), 20.5 (d, J = 18 Hz, P*C*H$_3$), 24.9 (t, J = 11 Hz, P*C*HCH$_3$), 27.9 (s, P*C*HCH$_3$), 124.2 (t, J = 3 Hz), 125.0 (s), 130.5 (t, J = 9 Hz,), 143.5 (t, J = 28 Hz), 159.6 (t, J = 24 Hz). ^{29}Si NMR (79 MHz, C_6D_6, 300 K, δ/ppm): 60.2 (m).

Synthesis of complex 2

Under 1 atm N_2, a solution of ligand **L2** (0.59 g, 1.2 mmol) in toluene (30 mL) was slowly added into the solution of Fe(PMe$_3$)$_4$ (0.45 g, 1.25 mmol) in toluene (30 mL) with stirring for 48 h at 45 °C, resulting in a dark yellow solution. After the reaction, the volatiles were removed and the remaining residue was extracted *via* *n*-pentane (60 mL) and diethyl ether (60 mL). The orange block crystals (complex **2**) were collected in a yield of 59%. Dec: >173 °C. Anal. Calc. for $C_{33}H_{51}FeN_2P_3Si$ (652.61 g mol^{-1}): C, 60.74; H, 7.88; N, 4.29. Found: C, 61.13; H, 8.06; N, 4.40. IR (Nujol mull, cm^{-1}): 2067 (N≡N), 1873 (Fe–H), 950 (PMe$_3$). ^{1}H NMR (300 MHz, C_6D_6, 300 K, δ/ppm): −14.44 (td, J = 72 Hz, 19 Hz, 1H, Fe–*H*), 0.88 (m, 6H, PCHC*H*$_3$), 0.94 (d, J = 6 Hz, 9H, PC*H*$_3$), 1.05 (m, 12H, PCHC*H*$_3$), 1.38 (m, 6H, PCHC*H*$_3$), 2.09–2.14 (m, 2H, PC*H*CH$_3$), 2.82 (m, 2H, PC*H*CH$_3$), 7.00 (m, 7H, Ar–*H*), 7.26 (d, J = 9 Hz, 2H, Ar–*H*), 7.37 (d, J = 6 Hz, 2H, Ar–*H*), 7.85 (d, J = 6 Hz, 2H, Ar–*H*). ^{31}P NMR (121 MHz, C_6D_6, 300 K, δ/ppm): 7.0 (t, J = 16 Hz, 1P, *P*Me$_3$), 93.5 (d, J = 16 Hz, 2P, *P*^{i}Pr$_2$). ^{13}C NMR (75 MHz, C_6D_6, 300 K, δ/ppm): 18.3 (s, PCH*C*H$_3$), 18.4 (t, J = 2 Hz, PCH*C*H$_3$), 19.8 (s, PCH*C*H$_3$), 20.9 (t, J = 2 Hz, PCH*C*H$_3$), 21.0 (d, J = 18 Hz, P*C*H$_3$), 28.5 (t, J = 12 Hz, P*C*HCH$_3$), 30.1 (s, P*C*HCH$_3$), 125.9 (t, J = 3 Hz), 126.7 (s), 126.8 (s), 127.0 (s), 128.3 (s), 133.4 (t, J = 9 Hz,), 137.2 (s), 147.0 (t, J = 25 Hz), 150.5 (s), 159.2 (t, J = 24 Hz). ^{29}Si NMR (79 MHz, C_6D_6, 300 K, δ/ppm): 65.9 (q, J = 32 Hz).

Synthesis of complex 3

Under atmospheric dinitrogen, a mixture of **L3** (0.27 g, 0.72 mmol) and Fe(PMe$_3$)$_4$ (0.26 g, 0.72 mmol) in toluene (50 mL) was stirred for 20 h at room temperature, obtaining a dark orange solution. After the reaction, the volatiles were removed and the remaining residue was extracted with *n*-pentane (60 mL) and diethyl ether (60 mL), respectively. The red orange crystals (complex **3**) were collected in 61% yield (0.27 g, 0.44 mmol). Dec: >152 °C. $C_{30}H_{47}FeN_2P_3Si$ (612.57 g mol^{-1}): C, 58.82; H, 7.73; N, 4.57. Found: C, 59.11; H, 7.60; N, 4.39. IR (Nujol mull, cm^{-1}): 2054 (N≡N), 1902 (Fe–H), 935 (PMe$_3$). ^{1}H NMR (300 MHz, C_6D_6, 300 K, δ/ppm): −11.23 (td, J = 64 Hz, 25 Hz, 1H, Fe–*H*), 1.03 (d, J = 6 Hz, 9H, PC*H*$_3$), 1.18 (m, 6H, PCHC*H*$_3$), 1.30 (d, J = 6 Hz, 9H, PC*H*$_3$), 1.46 (m, 6H, PCHC*H*$_3$), 2.56 (m, 2H, PC*H*CH$_3$), 7.11 (s, 4H), 7.33–7.68 (m, 8 H), 8.32 (d, J = 6 Hz, 2H). ^{31}P NMR (121 MHz, C_6D_6, 300 K, δ/ppm): 1.6 (t, J = 24 Hz, 1P, *P*Me$_3$), 22.9 (dd, J = 66 Hz, 24 Hz, 1P, *P*Me$_3$), 100.8 (dd, J = 66 Hz, 24.0 Hz, 1P, *P*^{i}Pr$_2$). ^{13}C NMR (75 MHz, C_6D_6, 300 K, δ/ppm): 20.0 (s, PCH*C*H$_3$), 20.3 (d, J = 3 Hz, PCH*C*H$_3$), 20.5 (s, PCH*C*H$_3$), 21.0 (d, J = 4 Hz, PCH*C*H$_3$), 21.2 (dd, J = 22 Hz, 2 Hz, P*C*H$_3$), 21.9 (dd, J = 22 Hz, 2 Hz, P*C*H$_3$), 30.1 (d, J = 8 Hz, P*C*HCH$_3$), 33.8 (dd, J = 26 Hz, 4 Hz, P*C*HCH$_3$), 126.1 (d, J = 4 Hz), 126.7 (s), 127.0 (d, J = 3 Hz), 127.2 (s), 128.5 (d, J = 2 Hz), 135.5 (s), 135.7 (s), 135.9 (s), 136.4 (s), 137.2 (s), 146.1 (s), 146.6 (s), 148.4 (s), 148.8 (d, J = 7 Hz), 149.4 (t, J = 3 Hz), 159.5 (d, J = 4 Hz), 160.2 (d, J = 4 Hz). ^{29}Si NMR (79 MHz, C_6D_6, 300 K, δ/ppm): 48.6 (m).

Synthesis of complex 4

Under atmospheric argon, the solution of **L3** (0.23 g, 0.61 mmol) in 30 mL of toluene was added into the solution of Fe(PMe$_3$)$_4$ (0.22 g, 0.61 mmol) in 30 mL of toluene with stirring for 20 h to afford a red orange solution at room temperature. The volatiles were removed *in vacuo* and the remaining residue was extracted with *n*-pentane (60 mL) and diethyl ether (60 mL), respectively. The dark orange crystals (complex **4**) were collected in 62% yield (0.73 g, 1.26 mmol). Dec: >148 °C. Anal. Calc. for $C_{30}H_{47}FeP_3Si$ (584.56 g mol^{-1}): C, 61.64; H, 8.10. Found: C, 61.49; H, 8.01. IR (Nujol mull, cm^{-1}): 1892 (Fe–H), 936 (PMe$_3$). ^{1}H NMR (300 MHz, C_6D_6, 300 K, δ/ppm): −12.42 (br, 1H, Fe–*H*), 0.90 (m, 6H, PCHC*H*$_3$), 1.13 (d, J = 6 Hz, 18H, PC*H*$_3$), 1.17 (s, 6H, PCHC*H*$_3$), 2.24 (br, 2H, PC*H*CH$_3$), 7.31–7.36 (m, 8H), 7.61 (br, 1H), 7.85 (d, J = 6 Hz, 1H), 7.96 (d, J = 7 Hz, 4H). ^{31}P NMR (121 MHz, C_6D_6, 300 K, δ/ppm): 22.9 (s, 2P, *P*Me$_3$), 112.6 (s, 1P, *P*^{i}Pr$_2$).

Synthesis of complex 5

The solution of complex **1** (0.8 g, 1.35 mmol) in 60 mL of THF was stirred under an atmosphere of hydrogen for 24 h at ambient temperature. The red solution was obtained after the reaction. The volatile components in the reaction mixture were evaporated *in vacuo* and the remaining residue was extracted with *n*-pentane (60 mL) and diethyl ether (60 mL). The yellow block crystals (complex **5**) were collected in a yield of 68% (0.52 g, 0.92 mmol) at −20 °C. Dec: >158.3 °C. Anal. Calc. for $C_{28}H_{51}FeP_3Si$ (564.57 g mol^{-1}): C, 59.57; H, 9.11. Found: C, 59.30; H, 9.02. IR (Nujol mull, cm^{-1}): 1919, 1835 (Fe–H), 946 (PMe$_3$). ^{1}H NMR (300 MHz, C_6D_6, 300 K, δ/ppm): −15.01 (br, 1H, Fe–H_c), −10.03 (br 2H, Fe–H_a and Fe–H_b), 0.46–0.53 (m, 6H, PCHC*H*$_3$), 0.57–0.64 (m, 6H, PCHC*H*$_3$), 0.71–0.76 (m, 6H, PCHC*H*$_3$), 0.89 (s, 3H, SiC*H*$_3$), 0.98 (d, J = 9 Hz, 9H, PC*H*$_3$), 1.04–1.07 (m, 6H, PCHC*H*$_3$), 1.47 (septet, J = 6 Hz, 2H, PC*H*CH$_3$), 2.32 (septet, J = 6 Hz, 2H, PC*H*CH$_3$), 6.79 (t, J = 9 Hz, 2H, Ar–*H*), 6.93 (t, J = 9 Hz, 2H, Ar–*H*), 7.00 (d, J = 9 Hz, 2H, Ar–*H*). 7.91 (d, J = 9 Hz, 2H, Ar–*H*). ^{31}P NMR (121 MHz, C_6D_6, 300 K, δ/ppm): 30.6 (t, J = 30 Hz, 1P, *P*Me$_3$), 121.0 (d, J = 30 Hz, 2P, *P*^{i}Pr$_2$). ^{13}C NMR (75 MHz, C_6D_6, 300 K, δ/ppm): 7.2 (s, Si–*C*H$_3$), 15.8 (t, J = 3 Hz, PCH*C*H$_3$), 17.4 (t, J = 3 Hz, PCH*C*H$_3$), 18.0 (s, PCH*C*H$_3$), 18.8 (t, J = 3 Hz, PCH*C*H$_3$), 23.0 (t, J = 14 Hz, P*C*HCH$_3$), 26.7 (dt, J = 22 Hz, 2 Hz, P*C*H$_3$), 27.3 (s, P*C*HCH$_3$), 124.3 (t, J = 2 Hz), 130.3 (t, J = 8 Hz,), 145.8 (d, J = 4 Hz), 146.1 (d, J = 2 Hz), 146.4 (d, J = 4 Hz), 158.6 (t, J = 20 Hz). ^{29}Si NMR (79 MHz, C_6D_6, 300 K, δ/ppm): 32.6 (m).

Synthesis of complex 6

A solution of complex **2** (0.78 g, 1.20 mmol) in 60 mL of THF was treated with H_2 (1 atm) with stirring for 24 h at room temperature, bringing about a gradual color change from

orange to red. The volatile components were removed *in vacuo* and the remaining residues were subsequently extracted with *n*-pentane (60 mL) and diethyl ether (60 mL) (3 × 20 ml) at room temperature. The yellow block crystals (complex **6**) were recrystallized in diethyl ether with a yield of 62% (0.47 g, 0.75 mmol) at −20 °C. Dec: >158.3 °C. Anal. Calc. for $C_{33}H_{53}FeP_3Si$ (626.64 g mol^{-1}): C, 63.25; H, 8.53. Found: C, 63.51; H, 8.39. IR (Nujol mull, cm^{-1}): 1916, 1819 (Fe–H), 946 (PMe_3). ^{1}H NMR (300 MHz, C_6D_6, 300 K, δ/ppm): −13.58 (br 1H, Fe–H_c), −9.10 (s 2H, Fe–H_a and Fe–H_b), 0.90–0.99 (m, 12H, PCHCH_3), 1.19–1.22 (m, 6H, PCHCH_3), 1.35 (d, J = 9 Hz, 9H, PCH_3), 1.38–1.47 (m, 6H, PCHCH_3), 1.93 (septet, J = 6 Hz, 2H, PCHCH$_3$), 2.72 (m, 2H, PCHCH$_3$), 7.15–7.47 (m), 8.15 (d, J = 6 Hz, 2H), 8.22 (d, J = 9 Hz, 2H). ^{31}P NMR (121 MHz, C_6D_6, 300 K, δ/ppm): 17.0 (t, J = 30 Hz, 1P, PMe$_3$), 107.2 (d, J = 30 Hz, 2P, P^iPr$_2$). ^{13}C NMR (75 MHz, C_6D_6, 300 K, δ/ppm): 17.2 (t, J = 3 Hz, PCHCH$_3$), 18.6 (t, J = 3 Hz, PCHCH$_3$), 19.2 (s, PCHCH$_3$), 20.8 (t, J = 3 Hz, PCHCH$_3$), 24.8 (t, J = 15 Hz, PCHCH$_3$), 27.3 (dt, J = 22 Hz, 2 Hz, PCH$_3$), 28.7 (s, PCHCH$_3$), 125.6 (t, J = 2 Hz), 127.1 (s), 127.2 (s), 133.1 (t, J = 8 Hz,), 135.9 (s), 148.2 (d, J = 4 Hz), 148.6 (d, J = 2 Hz), 148.8 (d, J = 4 Hz), 149.4 (d, J = 2 Hz), 158.1 (t, J = 20 Hz). ^{29}Si NMR (79 MHz, C_6D_6, 300 K, δ/ppm): 36.2 (dt, J = 21 Hz, 6 Hz).

Synthesis of complex 7

A solution of complex **3** (0.67 g, 1.10 mmol) in 60 mL of THF was treated with an atmospheric pressure of H_2. The mixture was stirred at room temperature for 24 h. The volatiles were evaporated to dryness *in vacuo* and the remaining residues were extracted with *n*-pentane (60 mL) and diethyl ether (3 × 20 ml) at room temperature. The yellow orange block crystals (complex **7**) were recrystallized in diethyl ether with a 62% yield (0.47 g, 0.75 mmol) at −20 °C. Dec: >159 °C. Anal. Calc. for $C_{30}H_{49}FeP_3Si$ (586.57 g mol^{-1}): C, 61.43; H, 8.42. Found: C, 61.25; H, 8.50. IR (Nujol mull, cm^{-1}): 1889, 1864 (Fe–H), 934 (PMe_3). ^{1}H NMR (300 MHz, C_6D_6, 300 K, δ/ppm): −12.46 (br, 3H, Fe–H), 0.90 (br, 6H, PCHCH_3), 1.13 (d, J = 6 Hz, 18H, PCH_3), 1.17 (br, 6H, PCHCH_3), 2.23 (br, 2H, PCHCH$_3$), 7.23–7.27 (m, 4H, Ar–H), 7.34 (t, J = 9 Hz, 4H, Ar–H), 7.60 (m, 1H, Ar–H), 7.85 (d, J = 6 Hz, 1H, Ar–H). 7.96 (d, J = 6 Hz, 4H, Ar–H). ^{31}P NMR (121 MHz, C_6D_6, 300 K, δ/ppm): 23.0 (s, 2P, PMe$_3$), 112.6 (s, 1P, P^iPr$_2$). ^{13}C NMR (75 MHz, C_6D_6, 300 K, δ/ppm): 18.3 (d, J = 2 Hz, PCHCH$_3$), 19.4 (s, PCHCH$_3$), 26.0 (d, J = 25 Hz, PCH$_3$), 27.9 (d, J = 20 Hz, PCHCH$_3$) 125.8 (d, J = 4 Hz), 127.0 (s), 134.6 (s), 134.9 (s), 135.9 (s), 148.4 (s), 145.0 (s), 158.3 (s), 159.0 (s). ^{29}Si NMR (79 MHz, C_6D_6, 300 K, δ/ppm): 31.9 (br).

X-ray crystal structure determination

Intensity data and cell parameters of complex **1** were recorded on a Stoe Stadi Vari diffractometer with graphite-monochromatized Cu Kα radiation (λ = 1.54186 Å) while the intensity data and cell parameters of complex **4** were recorded on a Stoe Stadi Vari diffractometer with Ga Kα radiation (λ = 1.34143 Å). Besides, the intensity data and cell parameters of complexes **2**, **3**, **5**, **6** and **7** were recorded on a Rigaku Oxford Diffraction XtaLAB Synergy-S diffractometer, employing a Cu Kα radiation source (λ = 1.54184 Å). Crystallographic data for complexes **1**, **2**, **3**, **4**, **5**, **6** and **7** are summarized in the ESI.† The structure was solved by direct methods and refined by full-matrix least-squares techniques against F^2 using the SHELXL program[23] through the OLEX interface.[24] All non-hydrogen atoms were refined anisotropically.

Catalytic reduction of dinitrogen to N(SiMe$_3$)$_3$

A typical procedure is described as follows. To a mixture of KC_8 and Me_3SiCl in solvent (20 mL) was added complex **3** (6.12 mg, 0.01 mmol) at 25 °C under N_2. After stirring for 20 h, to the reaction mixture was added *n*-dodecane as an internal standard. The insoluble substance was removed by centrifugation and the supernatant was used for GC analysis.

Conflicts of interest

There are no conflicts to declare.

Acknowledgements

This work was supported by the NSF China 21971151 and the major basic research project of Natural Science Foundation of Shandong Province ZR2019ZD46.

References

1 Y. Nishibayashi, *Inorg. Chem.*, 2015, **54**, 9234–9247.
2 N. Stucke, B. M. Flöser, T. Weyrich and F. Tuczek, *Eur. J. Inorg. Chem.*, 2018, 1337–1355.
3 (*a*) J. S. Anderson, J. Rittle and J. C. Peters, *Nature*, 2013, **501**, 84–88; (*b*) S. E. Creutz and J. C. Peters, *J. Am. Chem. Soc.*, 2014, **136**, 1105–1115; (*c*) Y. Sekiguchi, S. Kuriyama, A. Eizawa, K. Arashiba, K. Nakajima and Y. Nishibayashi, *Chem. Commun.*, 2017, **53**, 12040–12043; (*d*) S. E. Creutz and J. C. Peters, *J. Am. Chem. Soc.*, 2015, **137**, 7310–7313; (*e*) S. Kuriyama, K. Arashiba, K. Nakajima, Y. Matsuo, H. Tanaka, K. Ishii, K. Yoshizawa and Y. Nishibayashi, *Nat. Commun.*, 2016, **7**, 12181–12189; (*f*) G. Ung and J. C. Peters, *Angew. Chem., Int. Ed.*, 2015, **54**, 532–535; (*g*) P. J. Hill, L. R. Doyle, A. D. Crawford, W. K. Myers and A. E. Ashley, *J. Am. Chem. Soc.*, 2016, **138**, 13521–13524.
4 M. Yuki, H. Tanaka, K. Sasaki, Y. Miyake, K. Yoshizawa and Y. Nishibayashi, *Nat. Commun.*, 2012, **3**, 1254.
5 G. Ung and J. C. Peters, *Angew. Chem., Int. Ed.*, 2015, **54**, 532–535.
6 D. E. Prokopchuk, E. S. Wiedner, E. D. Walter, C. V. Popescu, N. A. Piro, W. S. Kassel, R. M. Bullock and M. T. Mock, *J. Am. Chem. Soc.*, 2017, **139**, 9291–9301.
7 (*a*) N. P. Mankad, M. T. Whited and J. C. Peters, *Angew. Chem., Int. Ed.*, 2007, **46**, 5768–5771; (*b*) M. T. Whited, N. P. Mankad, Y. Lee, P. F. Oblad and J. C. Peters, *Inorg. Chem.*, 2009, **48**, 2507–2517; (*c*) R. Imayoshi, K. Nakajima,

J. Takaya, N. Iwasawa and Y. Nishibayashi, *Eur. J. Inorg. Chem.*, 2017, 3769–3778.
8 R. B. Ferreira, B. J. Cook, B. J. Knight, V. J. Catalano, R. García-Serres and L. J. Murray, *ACS Catal.*, 2018, **8**, 7208–7212.
9 A. D. Piascik, R. Li, H. J. Wilkinson, J. C. Green and A. E. Ashley, *J. Am. Chem. Soc.*, 2018, **140**, 10691–10694.
10 S. Li, Y. Wang, W. Yang, K. Li, H. Sun, X. Li, O. Fuhr and D. Fenske, *Organometallics*, 2020, **39**, 757–766.
11 (*a*) J. Takaya, N. Kirai and N. Iwasawa, *J. Am. Chem. Soc.*, 2011, **133**, 12980–12983; (*b*) H. Fang, Y. K. Choe, Y. Li and S. Shimada, *Chem. – Asian J.*, 2011, **6**, 2512–2521; (*c*) J. Takaya, S. Nakamura and N. Iwasawa, *Chem. Lett.*, 2012, **41**, 967–969; (*d*) J. Zhu, Z. Lin and T. B. Marder, *Inorg. Chem.*, 2005, **44**, 9384–9390; (*e*) D. F. MacLean, R. McDonald, M. J. Ferguson, A. J. Caddell and L. Turculet, *Chem. Commun.*, 2008, 5146–5148.
12 Y. Bai, J. Zhang and C. Cui, *Chem. Commun.*, 2018, **54**, 8124–8127.
13 S. Wu, X. Li, Z. Xiong, W. Xu, Y. Lu and H. Sun, *Organometallics*, 2013, **32**, 3227–3237.
14 L. J. Murphy, M. J. Ferguson, R. McDonald, M. D. Lumsden and L. Turculet, *Organometallics*, 2018, **37**, 4814–4826.
15 L. Yang, D. R. Powell and R. P. Houser, *Dalton Trans.*, 2007, 955–964.
16 P. Zhang, X. Li, X. Qi, H. Sun, O. Fuhr and D. Fenske, *RSC Adv.*, 2018, **8**, 14092–14099.
17 (*a*) Y. Wang, Doctoral Dissertation, Shandong University, 2020; (*b*) Z. Xiong, X. Li, S. Zhang, Y. Shi and H. Sun, *Organometallics*, 2016, **35**, 357–363; (*c*) H. Zhang, Master Thesis, Shandong University, 2018.
18 S. Ren, S. Xie, T. Zheng, Y. Wang, S. Xu, B. Xue, X. Li, H. Sun, O. Fuhr and D. Fenske, *Dalton Trans.*, 2018, **47**, 4352–4359.
19 (*a*) F. Zhang, L. Wang, S. Chang, K. Huang, Y. Chi, W. Hung, C. Chen, G. Leed and P. Chou, *Dalton Trans.*, 2013, **42**, 7111–7119; (*b*) P. Zhang, Doctoral Dissertation, Shandong University, 2018.
20 S. Lachaize and S. Sabo-Etienne, *Eur. J. Inorg. Chem.*, 2006, **2006**, 2115–2127.
21 H. H. Karsch, *Chem. Ber.*, 1977, **110**, 2699–2711.
22 J. Kim, Y. Kim, I. Sinha, S. H. Kim and Y. Lee, *Chem. Commun.*, 2016, **52**, 9367–9370.
23 G. M. Sheldrick, *Acta Crystallogr., Sect. A: Found. Adv.*, 2015, **71**, 3–8.
24 O. V. Dolomanov, L. J. Bourhis, R. J. Gildea, J. A. K. Howard and H. Puschmann, *J. Appl. Crystallogr.*, 2009, **42**, 339–341.